THE JOURNAL OF PHYSICAL CHEMISTRY A

Article

pubs.acs.org/JPCA

Photoelectron Spectroscopic and Computational Study of Hydrated Pyrimidine Anions

John T. Kelly,[†] Shoujun Xu,[‡] Jacob Graham,[‡] J. Michael Nilles,[‡] Dunja Radisic,[‡] Angela M. Buonaugurio,[‡] Kit H. Bowen, Jr.,*[,‡] Nathan I. Hammer,*[,†] and Gregory S. Tschumper*[,†]

[†]Department of Chemistry and Biochemistry, University of Mississippi, P.O. Box 1848, University, Mississippi 38677, United States

[‡]Department of Chemistry, Johns Hopkins University, 3400 North Charles Street, Baltimore, Maryland 21218, United States

Supporting Information

ABSTRACT: The stabilization of the pyrimidine anion by the addition of water molecules is studied experimentally using photoelectron spectroscopy of mass-selected hydrated pyrimidine clusters and computationally using quantum-mechanical electronic structure theory. Although the pyrimidine molecular anion is not observed experimentally, the addition of a single water molecule is sufficient to impart a positive electron affinity. The sequential hydration data have been used to extrapolate to −0.22 eV for the electron affinity of neutral pyrimidine, which agrees very well with previous observations. These results for pyrimidine are consistent with previous studies of the hydrated cluster anions of uridine, cytidine, thymine, adenine, uracil, and naphthalene. This commonality suggests a universal effect of sequential hydration on the electron affinity of similar molecules.

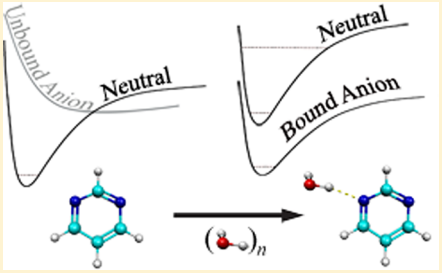

INTRODUCTION

The interaction of low-energy electrons with nucleic acid bases as a result of interactions with ionizing radiation is known to induce the fragmentation of DNA.[1] Much effort has been made to elucidate the mechanisms at play and the specific sites at which fragmentation occurs.[2−4] There is evidence that suggests that pyrimidine nucleobases are sites at which an excess electron can be localized. Pyrimidine is a nitrogen-containing heterocyclic molecule that serves as a structural motif in many important biological molecules. Besides being incorporated in uracil and thymine nucleic acid bases, it is also present in many natural products (e.g., vitamin B_1), synthetic products, and so on.

Pyrimidine is known to possess a negative electron affinity (EA).[5] Anions created from such molecules, whose energies are higher than those of their neutral counterparts, are unstable with respect to autodetachment. However, the interaction of electrons with isolated neutral molecules having negative adiabatic electron affinities can produce short-lived, "temporary" anions in the gas phase[6,7] and actually become stable in the condensed phase. This phenomenon suggests that interactions between the unbound ion and solvent molecules stabilize the excess charge and lowers the energy of the anion below that of the corresponding neutral. From an energetic standpoint, the interaction of an anion with one or more neutral solvent molecules is more favorable than the interaction of that ion's neutral counterpart with an equal number of those same solvent molecules.

The stabilization of the pyrimidine anion by interactions with different solvent species has previously been investigated by Periquet et al.[8] The addition of six argon, five krypton, or four xenon atoms resulted in a stable anion, as did the addition of one water, two ammonia, or three toluene molecules. These results suggest that the magnitude of the EA of the unstable pyrimidine anion is a small negative value. Electron transmission spectroscopic results from the mid-1970s also suggest that the pyrimidine anion has an EA close to zero, possibly down as far as −0.25 eV.[5]

Here we use negative ion photoelectron spectroscopy to quantify the stabilization effect that water has on the otherwise unstable pyrimidine anion. This solvent-induced anion stabilization has been observed in similar molecules including uridine, cytidine, thymine, adenine, uracil, and naphthalene.[9−14] When studying solvent stabilization effects on unstable anions, mass analysis allows for the systematic addition of solvent molecules, along with the determination of the minimum number of solvent molecules necessary to stabilize the negative ion. Analysis of photoelectron spectra of solvated cluster anions also offers a direct method of measuring the stabilization of the anion by interrogation of the EAs of the clusters.

EXPERIMENTAL METHODS

Negative ion photoelectron spectroscopy is conducted by crossing the mass-selected negative ion beam with a fixed frequency laser and energy analyzing the resulting photodetached electrons. This process is governed by the equation:

$$h\nu = \mathrm{EKE} + \mathrm{EBE} \quad (1)$$

Special Issue: David R. Yarkony Festschrift

Received: May 13, 2014
Revised: June 16, 2014
Published: June 17, 2014

where EKE is the electron kinetic energy and EBE is the electron binding energy. The negative ion photoelectron spectrometer at Johns Hopkins University has been described previously.[15] Anions were formed at its supersonic expansion source. There, the mixture of pyrimidine and water was heated to ∼60 °C and expanded together with argon gas through the 20 μm nozzle orifice. The low-energy electrons from a biased filament were injected into the expanding jet in the presence of a weak magnetic field. The apparatus utilized a Wien filter for mass selection. A magnetic sector mass spectrometer was also used for mass analysis. Photodetachment was accomplished with 2.54 eV (488 nm) photons of an intracavity laser. Photodetached electrons were analyzed with a hemispherical electron energy analyzer with a typical resolution of ∼25 meV. The well-known photoelectron spectra of O^- and NO^- were used for calibration.[16−18]

COMPUTATIONAL METHODS

Full geometry optimizations and harmonic vibrational frequency calculations were performed on all hydrated pyrimidine cluster anion structures using the spin-unrestricted UB3LYP density functional theory (DFT) method[19−21] and 6-31++G(2df,2pd) double-ζ basis set as implemented in the Gaussian 09 software package.[22] Pure angular momentum (5d,7f) atomic orbital basis functions were utilized rather than the Cartesian counterparts (6d,10f). A pruned numerical integration grid composed of 99 radial shells and 590 angular points per shell was employed with a threshold of 10^{-10} for the RMS change in the density matrix during the self-consistent field procedure. The maximum Cartesian force for each optimized structure did not exceed 1.4×10^{-6} Hartrees/Bohr. Our previous optimized neutral pyrimidine/water structures[23] were taken as starting geometries for the $[Py\cdot(H_2O)_n]^-$ (n = 1−5) anions. Additional starting structures were created by taking known hydrated electron cluster geometries $[(H_2O)_n^-]$[24−27] and attaching a pyrimidine molecule to a free hydrogen atom via an HOH···N hydrogen bond. Although this procedure is by no means an exhaustive exploration of the complicated potential energy surfaces associated with these clusters, it should, at the very least, identify representative minima close to the global minimum.

Vertical detachment energies (VDEs) of low-lying UB3LYP optimized structures were calculated as the difference between the electronic energy anion and that of the corresponding neutral species (constrained to the anion geometry). All computations used to determine VDEs employed the same 6-31+G(2df,2pd) basis set. The electronic energies of the neutral clusters were computed with the spin-restricted RB3LYP DFT method.

The optimized geometries and harmonic frequencies of the corresponding neutral clusters were also computed with the spin-restricted RB3LYP DFT method and the 6-31++G-(2df,2pd) basis set to evaluate the adiabatic electron affinities (AEAs) of the $Py\cdot(H_2O)_n$ series. To preserve the hydrogen bonding motifs and minimize solvent reorganization, we used the optimized anion structures as starting points for subsequent geometry optimizations of the neutral clusters. These neutral structures were all identified in our previous work[23] but do not necessarily correspond to the lowest-energy configuration. AEAs corrected for the zero-point vibrational energy (ZPVE) of both the anion and neutral were also determined from the unscaled B3LYP/6-31++G(2df,2pd) harmonic vibrational frequencies. Extensive calibration[28] has determined the electron affinities computed with the B3LYP DFT method, and a comparable double-ζ basis set is typically within four tenths of an electronvolt of the experimental values for valence bound anions.

EXPERIMENTAL RESULTS

Figure 1 shows a typical mass spectrum of the pyrimidine/water cluster anion system. The first observed member of the

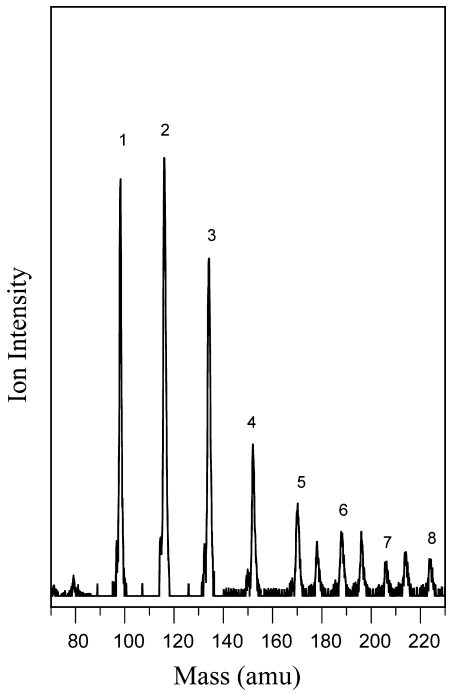

Figure 1. Mass spectrum of $[Py\cdot(H_2O)_n]^-$ cluster anions, n = 1−8.

$[Py\cdot(H_2O)_n]^-$ series is the $[Py\cdot(H_2O)]^-$ anion. The pyrimidine molecular anion was not observed. This result suggests that just one water molecule was sufficient to stabilize negative ion of pyrimidine, in agreement with the previous results of Periquet et al.[8] The intensity of the second member of the series, $[Py\cdot(H_2O)_2]^-$, is stronger than that of $[Py\cdot(H_2O)]^-$, which is a characteristic common to all of the solvent-stabilized systems we have previously studied.[9−14] The first solvent-stabilized cluster in the series is likely to be only weakly bound, and this low stability is manifested by the weaker signal in the mass spectrum. The intensity of the hydrated series decreases sharply after n = 2 but levels off after n = 5. $[Py_2\cdot(H_2O)_m]^-$ clusters can also be seen in our mass spectrum between the peaks for $n = m + 4$ and $n = m + 5$ (e.g., $[Py_2\cdot(H_2O)_2]^-$ between n = 6, 7) Intensities of these clusters containing two or more pyrimidine molecules are significantly weaker compared with the largest peaks associated with the $[Py\cdot(H_2O)]^-$ clusters. As such, clusters containing more than one pyrimidine will not be discussed or analyzed here.

The photoelectron spectra of the first eight members of the hydrated series $[Py\cdot(H_2O)_n]^-$ are presented in Figure 2. The experimental threshold energies (E_{th}) and EAs are presented in Table 1, along with the stepwise increase in the EAs with sequential hydration (ΔEA). The spectra have very broad features, typical of solvated valence anions. The spectral profile is conserved through the series, but there is a nonlinear shift to higher binding energies and additional broadening with

dx.doi.org/10.1021/jp504724v | J. Phys. Chem. A 2014, 118, 11901−11907

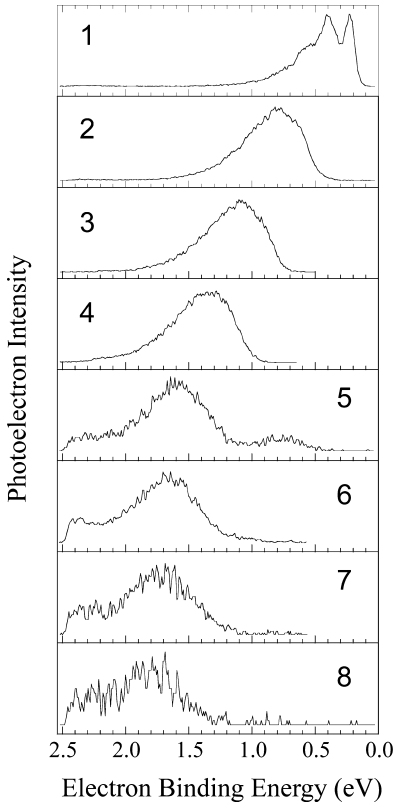

Figure 2. Photoelectron spectra of $[Py{\cdot}(H_2O)_n]^-$, n = 1−8 cluster anions recorded with 2.54 eV photons.

Table 1. Experimental Electron Affinities (EAs) of Hydrated Pyrimidine Clusters $[Py{\cdot}(H_2O)_n]^-$, Their Stepwise Increase ($\Delta EA = EA_n - EA_{n-1}$), and the Threshold Energies (E_{th}) of Their Negative Ion Photoelectron Spectra[a]

n	E_{th}	EA	ΔEA
1	0.10	0.23	
2	0.32	0.62	0.39
3	0.64	0.93	0.29
4	0.87	1.16	0.23
5	1.04	1.36	0.20
6	1.10	1.45	0.09
7	1.11	1.51	0.06
8	1.17	1.59	0.08

[a]All energy values are in electronvolts.

increasing cluster size. The first member of the series (n = 1) is characterized with two peaks at 0.23 and 0.41 eV. We assigned the lower binding energy peak as a transition origin, taking the center of this peak as an experimental EA of $Py{\cdot}(H_2O)$ cluster. The spacing between the origin transition and the higher energy peak (~1449 ± 80 cm^{-1}) indicates that the higher binding energy peak could be caused by the vibrations of pyrimidine.[29−35] We assigned the EBEs of the next five members of the hydrated series by comparing and overlaying the adjacent pairs of the series, n = 1, n = 2, and n = 3, and so on. This procedure has proven to be fairly reliable in the systems we have previously studied.[13,14] In the photoelectron spectrum of $[Py{\cdot}(H_2O)_5]^-$ negative ion, there is an additional broad feature around 0.75 eV. A summary of these results is presented in Table 1.

RESULTS: COMPUTATIONAL

Figure 3 shows select optimized structures for low-energy $[Py{\cdot}(H_2O)_n]^-$ (n = 1−5) cluster anions identified in this study, and

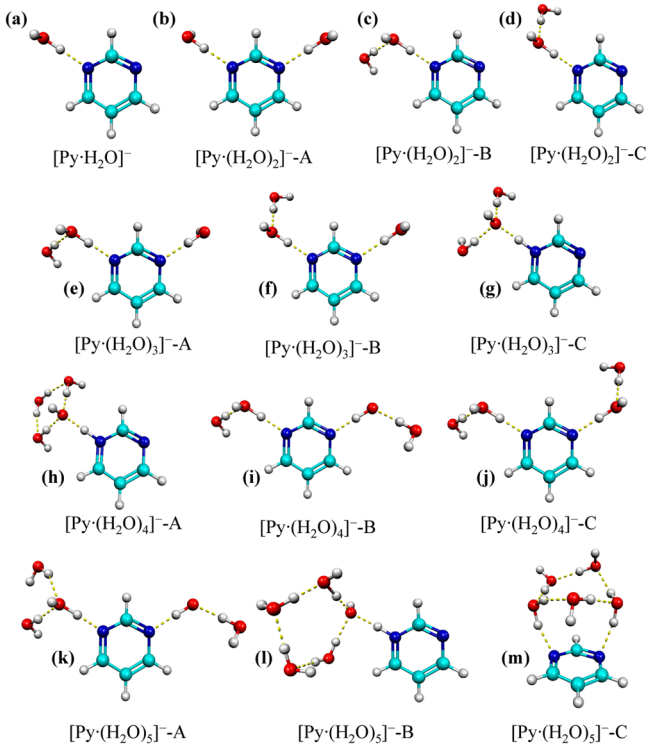

Figure 3. Structures of select $[Py{\cdot}(H_2O)_n]^-$ (n = 1−5) cluster anions optimized at the B3LYP/6-31++G(2df,2pd) level of theory.

Table 2. Vertical Detachment Energies for Select $[Py{\cdot}(H_2O)_n]^-$ (n = 1−5) Cluster Anions and Adiabatic Electron Affinities of the Corresponding Neutral Clusters Calculated Using B3LYP/6-31++G(2df,2pd) Level of Theory

	VDE	AEA	AEA^0
$[Py{\cdot}H_2O]^-$	0.43	0.14	0.28
$[Py{\cdot}(H_2O)_2]^-$-A	0.91	0.56	0.69
$[Py{\cdot}(H_2O)_2]^-$-B	0.77	0.29	0.46
$[Py{\cdot}(H_2O)_2]^-$-C	0.77	0.34	0.51
$[Py{\cdot}(H_2O)_3]^-$-A	1.22	0.68	0.83
$[Py{\cdot}(H_2O)_3]^-$-B	1.21	0.68	0.83
$[Py{\cdot}(H_2O)_3]^-$-C	1.99	0.44	0.63
$[Py{\cdot}(H_2O)_4]^-$-A	2.34	0.88	1.03
$[Py{\cdot}(H_2O)_4]^-$-B	1.50	0.78	0.96
$[Py{\cdot}(H_2O)_4]^-$-C	1.50	0.78	0.95
$[Py{\cdot}(H_2O)_5]^-$-A	1.74	0.85	1.03
$[Py{\cdot}(H_2O)_5]^-$-B	2.17	0.65	0.84
$[Py{\cdot}(H_2O)_5]^-$-C	0.99	0.47	0.58

Table 2 lists their computed vertical detachment energies (VDEs) for the anions and AEAs with (AEA^0) and without (AEA) the zero-point vibrational energy corrections for the corresponding neutrals. Only a single low-energy $[Py{\cdot}(H_2O)]^-$ minimum was found (Figure 3a), and it is characterized by a OH···N hydrogen bond donated from water to pyrimidine. The VDE of this structure was found to be 0.43 eV, while corresponding neutral has an AEA and AEA^0 of 0.14 and 0.28

dx.doi.org/10.1021/jp504724v | J. Phys. Chem. A 2014, 118, 11901−11907

eV, respectively. The latter value is slightly larger than the lowest energy experimental feature at 0.22 eV but smaller than the second lowest experimental feature at 0.41 eV. The magnitude of the corrections for the ZPVE is essentially the same for all of the clusters examined in this work. The AEA^0 is consistently 0.14 to 0.19 eV larger than the AEA, and, as such, the latter quantity is largely omitted from the remaining discussion.

The three lowest-lying $[Py\cdot(H_2O)_2]^-$ minimum energy structures identified on the B3LYP/6-31++G(2df,2pd) potential energy surface are shown in Figure 3b–d. The lowest energy structure (Figure 3b) has water molecules donating hydrogen bonds to each of the nitrogen atoms of the pyrimidine ring and exhibits a VDE of 0.91 eV, while the analogous neutral has an AEA^0 of 0.69 eV. The two other low-energy $[Py\cdot(H_2O)_2]^-$ isomers (Figure 3c,d) share the same structural motif where a water dimer is hydrogen-bonded to one of the nitrogen atoms (i.e., both waters on the same side of the pyrimidine ring). Both structures are 2.6 kcal mol^{-1} higher in energy than $[Py\cdot(H_2O)_2]^-$-A according to the B3LYP/6-31++G(2df,2pd) electronic energies. These two structures have identical VDEs of 0.77 eV but slightly different corresponding neutral AEA^0 values (0.46 eV for $[Py\cdot(H_2O)_2]^-$-B and 0.51 eV for $[Py\cdot(H_2O)_2]^-$-C). These calculated values agree very well with experiment (0.62 eV) and suggest that multiple structural isomers could be present experimentally. No anion structures were found that form cyclic hydrogen bonding networks involving both CH···O and OH···N interactions as previously identified for neutral $Py\cdot(H_2O)_2$ clusters.[23]

Several $[Py\cdot(H_2O)_3]^-$ minima were identified. The two lowest energy structures, $[Py\cdot(H_2O)_3]^-$-A and $[Py\cdot(H_2O)_3]^-$-B, are nearly isoenergetic and are shown in Figure 3e,f, respectively. These structures essentially have a water dimer hydrogen bonded to one nitrogen atom and a water monomer donating a hydrogen bond to the other nitrogen atom of the pyrimidine ring. Some higher energy structures were identified that exhibit proton transfer from water to pyrimidine, such as $[Py\cdot(H_2O)_3]^-$-C in Figure 3g. Additional structures with all three water molecules on the same side of the ring and interacting with just one nitrogen atom (not shown) were identified and found to be appreciably higher in energy. The VDE and AEA^0 for the corresponding neutral computed for $[Py\cdot(H_2O)_3]^-$-A are 1.22 and 0.83 eV, respectively. The values of those for $[Py\cdot(H_2O)_3]^-$-B are virtually identical (within 0.01 eV), and both values agree very well with the experimental EA of 0.93 eV. The structure that exhibits proton transfer, $[Py\cdot(H_2O)_3]^-$-C, is only 1.8 kcal mol^{-1} higher in energy than the other two isomers at the B3LYP/6-31++G(2df,2pd) level of theory. Its VDE is much higher at 1.99 eV, while the AEA^0 of the analogous neutral is 0.63 eV due to significant rearrangement upon the loss of the excess electron.

Over 20 $[Py\cdot(H_2O)_n]^-$ (n = 4,5) minima were identified that exhibit structural motifs similar to these observed for the smaller hydrated structures. For n = 4, the two lowest energy structures that were found are structurally similar and exhibit proton transfer from water to pyrimidine, as shown by $[Py\cdot(H_2O)_4]^-$-A in Figure 3h. The VDE and AEA^0 of the neutral for this structure are 2.34 and 1.03 eV, respectively, compared with an experimental EA value of 1.16 eV. The two structures $[Py\cdot(H_2O)_4]^-$-B and $[Py\cdot(H_2O)_4]^-$-C lie within <1 kcal mol^{-1} according to B3LYP/6-31++G(2df,2pd) electronic energies (Figure 3i,j, respectively). These two structures are characterized by a pair of water dimers donating a single hydrogen bond to one of the nitrogen atoms in pyrimidine. The VDE and AEA^0 of the corresponding neutral are 1.50 and 1.03 eV for $[Py\cdot(H_2O)_4]^-$-B, respectively, and those for $[Py\cdot(H_2O)_4]^-$-C differ by no more than 0.01 eV. All of these AEA^0 values are similar to the experimental EA of 1.16 eV, and these B3LYP computations suggest that either structural motif could be present in the experiment.

The lowest energy $[Py\cdot(H_2O)_5]^-$ structure ($[Py\cdot(H_2O)_5]^-$-A) that was identified is shown in Figure 3k and exhibits a water dimer hydrogen bonded to one nitrogen atom of the pyrimidine ring and a water trimer cluster hydrogen bonded to the other nitrogen atom. The computed VDE and AEA^0 for the corresponding neutral are 1.74 and 1.03 eV, which agree with the experimental EA of 1.36 eV. Penta-hydrated structures exhibiting proton transfer such as $[Py\cdot(H_2O)_5]^-$-B in Figure 3l were also found. $[Py\cdot(H_2O)_5]^-$-B is <1 kcal mol^{-1} higher in energy than $[Py\cdot(H_2O)_5]^-$-A at the B3LYP/6-31++G(2df,2pd) level of theory and has a VDE of 2.17 eV and a AEA^0 of 0.84 eV for the analogous neutral. Figure 3m shows a higher energy $[Py\cdot(H_2O)_5]^-$ isomer that is characterized by a cyclic water pentamer ring hydrogen bonded to both of pyrimidine's nitrogen atoms. $[Py\cdot(H_2O)_5]^-$-C is the lowest energy isomer identified that displays this structural motif. Although it is 3.9 kcal mol^{-1} higher in energy than $[Py\cdot(H_2O)_5]^-$-A at this level of theory, it has a calculated VDE of 0.99 and AEA^0 of 0.58 eV for the related neutral that could account for the experimental feature at 0.80 eV in the experimental spectrum of $[Py\cdot(H_2O)_5]^-$.

Interestingly, the hydrogen bonding motifs of the lowest energy $[Py\cdot(H_2O)_n]^-$ structures identified in this work are somewhat different than for their neutral counterparts. The lowest-energy neutral $Py\cdot(H_2O)_n$ clusters prefer to have all of the water molecules on one side of the pyrimidine ring, interacting with only one of the nitrogen atoms.[23] In contrast, the lowest-energy anions identified in this study lead to either the water molecules interacting with both nitrogen atoms of the pyrimidine ring or aggregating to donate a proton to one of the nitrogen atoms in the ring.

DISCUSSION

The electron affinity of the $[Py\cdot(H_2O)_n]$ series increases with increasing n, and this can be described with the thermodynamic cycle

$$EA[X(Y)_n] = EA[X] + \sum_{m=0}^{n-1} D_0[X(Y)_m\cdots Y] - \sum_{m=0}^{n-1} D_0[X(Y)_m\cdots Y] \quad (2)$$

where X represents the solvated molecule of interest, Y represents the solvent, $D_0[X^-(Y)_m\cdots Y]$ is the ion-neutral dissociation energy for the loss of one solvent molecule from the anion cluster, and $D_0[X(Y)_m\cdots Y]$ is the neutral–neutral dissociation energy for the loss of one solvent molecule from the neutral cluster. This description relies on the condition that the excess electron in the $[Py\cdot(H_2O)_n]^-$ clusters is primarily localized on pyrimidine in valence bound orbitals and not delocalized to any great extent in the solvent network. From eq 2, the sequential energy change per solvent molecule can be expressed as

$$\Delta EA = EA[X(Y)_n] - EA[X(Y)_{n-1}] = D_0[X(Y)_{n-1}\cdots Y] - D_0[X(Y)_{n-1}\cdots Y] \quad (3)$$

dx.doi.org/10.1021/jp504724v | J. Phys. Chem. A 2014, 118, 11901–11907

Negative ion photoelectron spectroscopy can therefore yield the necessary information for the quantization of the energy change for solvation if the excess electron is not significantly interacting with the solvent network.

The solvation of pyrimidine with one water molecule results in a positive electron affinity.[8] Additional water molecules to the cluster stabilize the excess charge and increase the electron affinity of the pyrimidine monomer in a predictable trend, as shown in Figure 4. Using eqs 2 and 3, extrapolation of the

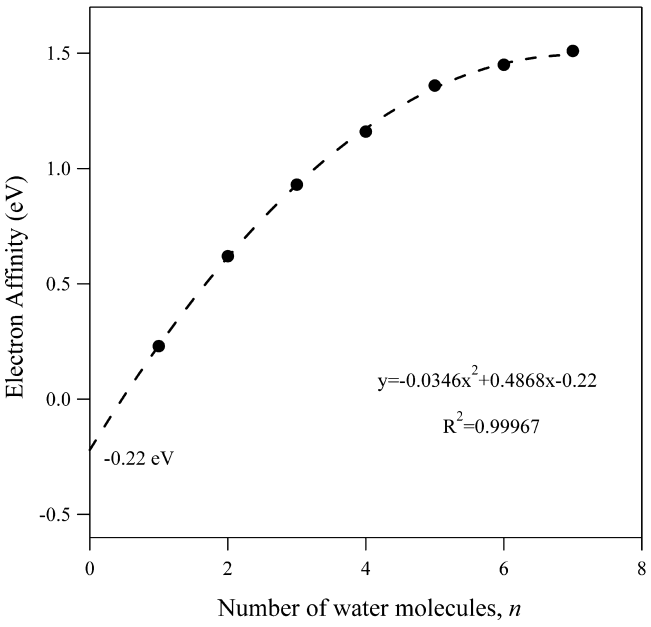

Figure 4. Plot of the experimental electron affinities (EAs) of hydrated pyrimidine clusters as a function of cluster size, *n*.

electron affinity as a function of the number of water molecules back to $n = 0$ yields the electron affinity of the pyrimidine monomer to be −0.22 eV. This approximation agrees very well with the previous electron transmission spectroscopic measurement in the vicinity of −0.25 eV.[5] Figure 5 quantifies the change in electron affinity (ΔEA) with each additional water molecule added. The first water molecule addition has the largest impact on the anion cluster going from −0.22 to 0.21 eV, a 0.43 eV difference, but as the number of water molecules increases the ΔEA decreases. These results are consistent with those for uridine, cytidine, thymine, adenine, uracil, and naphthalene.[9−14] In each of these systems, the sequential addition of water molecules increases the electron binding energy of the cluster, with the first water molecule having the largest impact on the electron affinity. In the cases of uridine, cytidine, thymine, adenine, and uracil, molecular anions exist, and hydration serves to increase the electron binding energy of the negatively charged cluster. The case of naphthalene, however, is nearly identical to pyrimidine in that although the neutral molecule has a negative electron affinity, the addition of one water molecule creates a stable negative ion.[14]

Interestingly, the computational results reveal that the localization of excess charge in the $[Py{\cdot}(H_2O)_n]^-$ cluster anions does not change appreciably with increasing *n*. Starting with the smallest experimentally observed pyrimidine anion cluster, $[Py{\cdot}(H_2O)]^-$, B3LYP computations show the excess electron residing in a singly occupied molecular orbital (SOMO) that is characterized as a valence π^* orbital on

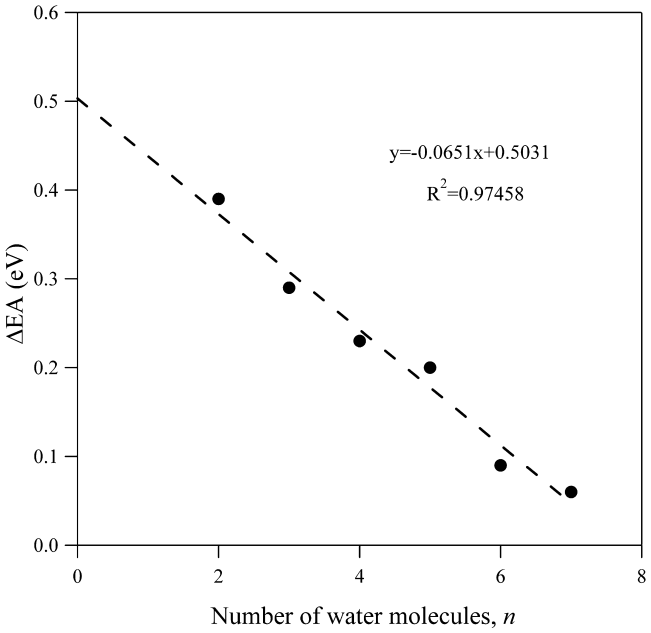

Figure 5. Plot of the sequential spectral shifts (ΔEA) of $[Py{\cdot}(H_2O)_n]^-$ photoelectron spectra as a function of cluster size, *n*.

pyrimidine. This character does not change with increasing *n* even though the photoelectron spectra evolve to more closely resemble that of bulk water.[36] This suggests that the addition of subsequent water molecules simply increases the overall electron binding energy of the entire anionic cluster.[14]

CONCLUSIONS

Although the pyrimidine molecular anion is shown to be energetically unstable, only a single water molecule is required to stabilize a negative ion state. B3LYP computations indicate that the excess electron primarily resides in a pyrimidine antibonding π^* orbital, and the character of this SOMO does not change appreciably even after the addition of five water molecules. This localization of excess charge on pyrimidine allows us to extrapolate the electron affinity of the pyrimidine monomer out to −0.22 eV, which is in good agreement with a previous experimental estimate. The addition of the first water molecule has the largest impact on the electron affinity of the cluster, in agreement with our previous results for uridine, cytidine, thymine, adenine, uracil, and naphthalene.[9−14] Although agreement between experimental PES spectra and our theoretical predictions is very good, infrared spectroscopic studies of $[Py{\cdot}(H_2O)_n]^-$ clusters would provide much insight into the structural motifs of the anion clusters present in the experiment.

ASSOCIATED CONTENT

Supporting Information

Cartesian coordinates, experimental photoelectron spectra of hydrated pyrimidine dimer clusters, experimental electron affinities and vertical detachment energies values extracted from experimental photoelectron spectra of hydrated pyrimidine dimer clusters, images of optimized neutral hydrated pyrimidine molecular clusters, and singly occupied molecular orbital images of select optimized hydrated pyrimidine cluster anions. This material is available free of charge via the Internet at http://pubs.acs.org.

AUTHOR INFORMATION

Corresponding Authors

*K.H.B.: E-mail: kbowen@jhu.edu.
*N.I.H.: E-mail: nhammer@olemiss.edu.
*G.S.T.: E-mail: tschumpr@olemiss.edu.

Notes

The authors declare no competing financial interest.

ACKNOWLEDGMENTS

This material is partially based (experimental) on work supported by the National Science Foundation under grant nos. CHE-1111693 and CHE-1360692 (K.H.B.). This material is partially based (computational) on work supported by the National Science Foundation under grant no. CHE-0957317 (G.S.T.). This material is partially based (computational) on work supported by the National Science Foundation under grant no. CHE-0955550 (N.I.H.). Both G.S.T. and N.I.H. acknowledge EPSCoR support under grant no. EPS-0903787.

REFERENCES

(1) Boudaïffa, B.; Cloutier, P.; Hunting, D.; Huels, M. A.; Sanche, L. Resonant Formation of DNA Strand Breaks by Low-Energy (3 to 20 eV) Electrons. *Science* **2000**, *287* (5458), 1658−1660.

(2) Bao, X.; Wang, J.; Gu, J.; Leszczynski, J. DNA strand breaks induced by near-zero-electronvolt electron attachment to pyrimidine nucleotides. *Proc. Natl. Acad. Sci. U. S. A.* **2006**, *103* (15), 5658−5663.

(3) Gu, J.; Wang, J.; Leszczynski, J. Electron Attachment-Induced DNA Single Strand Breaks: C3′−O3′ σ-Bond Breaking of Pyrimidine Nucleotides Predominates. *J. Am. Chem. Soc.* **2006**, *128* (29), 9322−9323.

(4) Gu, J.; Xie, Y.; Schaefer, H. F. Glycosidic Bond Cleavage of Pyrimidine Nucleosides by Low-Energy Electrons: A Theoretical Rationale. *J. Am. Chem. Soc.* **2004**, *127* (3), 1053−1057.

(5) Nenner, I.; Schulz, G. Temporary negative ions and electron affinities of benzene and N-heterocyclic molecules: pyridine, pyridazine, pyrimidine, pyrazine, and s-triazine. *J. Chem. Phys.* **1975**, *62* (5), 1747−1758.

(6) Aflatooni, K.; Gallup, G. A.; Burrow, P. D. Electron Attachment Energies of the DNA Bases. *J. Phys. Chem. A* **1998**, *102* (31), 6205−6207.

(7) Jordan, K. D.; Burrow, P. D. Studies of the temporary anion states of unsaturated hydrocarbons by electron transmission spectroscopy. *Acc. Chem. Res.* **1978**, *11* (9), 341−348.

(8) Periquet, V.; Moreau, A.; Carles, S.; Schermann, J. P.; Desfrançois, C. Cluster size effects upon anion solvation of N-heterocyclic molecules and nucleic acid bases. *J. Electron Spectrosc. Relat. Phenom.* **2000**, *106* (2−3), 141−151.

(9) Eustis, S.; Wang, D.; Lyapustina, S.; Bowen, K. H. Photoelectron spectroscopy of hydrated adenine anions. *J. Chem. Phys.* **2007**, *127* (22), 224309 .

(10) Headrick, J. M. Ph.D. Dissertation, Johns Hopkins University, Baltimore, MD, 1996.

(11) Hendricks, J. H.; Lyapustina, S. A.; de Clercq, H. L.; Bowen, K. H. The dipole bound-to-covalent anion transformation in uracil. *J. Chem. Phys.* **1998**, *108* (1), 8−11.

(12) Hendricks, J. H.; Lyapustina, S. A.; de Clercq, H. L.; Snodgrass, J. T.; Bowen, K. H. Dipole bound, nucleic acid base anions studied via negative ion photoelectron spectroscopy. *J. Chem. Phys.* **1996**, *104* (19), 7788−7791.

(13) Lyapustina, S. A. Ph.D. Dissertation, Johns Hopkins University, Baltimore, MD, 1999.

(14) Lyapustina, S. A.; Xu, S.; Nilles, J. M.; Bowen, K. H. Solvent-induced stabilization of the naphthalene anion by water molecules: A negative cluster ion photoelectron spectroscopic study. *J. Chem. Phys.* **2000**, *112* (15), 6643−6648.

(15) Coe, J. V.; Snodgrass, J. T.; Freidhoff, C. B.; McHugh, K. M.; Bowen, K. H. Photoelectron spectroscopy of the negative ion SeO^-. *J. Chem. Phys.* **1986**, *84* (2), 618−625.

(16) Neumark, D. M.; Lykke, K. R.; Andersen, T.; Lineberger, W. C. Laser photodetachment measurement of the electron affinity of atomic oxygen. *Phys. Rev. A* **1985**, *32* (3), 1890−1892.

(17) Siegel, M. W.; Celotta, R. J.; Hall, J. L.; Levine, J.; Bennett, R. A. Molecular Photodetachment Spectrometry. I. The Electron Affinity of Nitric Oxide and the Molecular Constants of NO-. *Phys. Rev. A* **1972**, *6* (2), 607−631.

(18) Travers, M. J.; Cowles, D. C.; Ellison, G. B. Reinvestigation of the electron affinities of O2 and NO. *Chem. Phys. Lett.* **1989**, *164* (5), 449−455.

(19) Becke, A. D. A multicenter numerical integration scheme for polyatomic molecules. *J. Chem. Phys.* **1988**, *88* (4), 2547−2553.

(20) Becke, A. D. Density-functional thermochemistry. III. The role of exact exchange. *J. Chem. Phys.* **1993**, *98* (7), 5648−5652.

(21) Lee, C.; Yang, W.; Parr, R. G. Development of the Colle-Salvetti correlation-energy formula into a functional of the electron density. *Phys. Rev. B* **1988**, *37* (2), 785−789.

(22) Frisch, M.; Trucks, G.; Schlegel, H.; Scuseria, G.; Robb, M.; Cheeseman, J.; Scalmani, G.; Barone, V.; Mennucci, B.; Petersson, G. *Gaussian 09*, revision A. 1; Gaussian, Inc: Wallingford, CT, 2009.

(23) Howard, J. C.; Hammer, N. I.; Tschumper, G. S. Structures, Energetics and Vibrational Frequency Shifts of Hydrated Pyrimidine. *ChemPhysChem* **2011**, *12* (17), 3262−3273.

(24) Hammer, N. I.; Roscioli, J. R.; Johnson, M. A. Identification of Two Distinct Electron Binding Motifs in the Anionic Water Clusters: A Vibrational Spectroscopic Study of the $(H_2O)_6^-$ Isomers. *J. Phys. Chem. A* **2005**, *109* (35), 7896−7901.

(25) Hammer, N. I.; Roscioli, J. R.; Johnson, M. A.; Myshakin, E. M.; Jordan, K. D. Infrared Spectrum and Structural Assignment of the Water Trimer Anion†. *J. Phys. Chem. A* **2005**, *109* (50), 11526−11530.

(26) Hammer, N. I.; Shin, J.-W.; Headrick, J. M.; Diken, E. G.; Roscioli, J. R.; Weddle, G. H.; Johnson, M. A. How Do Small Water Clusters Bind an Excess Electron? *Science* **2004**, *306* (5696), 675−679.

(27) Lee, H. M.; Lee, S.; Kim, K. S. Structures, energetics, and spectra of electron−water clusters, $e^-(H_2O)_{2-6}$ and $e^-HOD(D_2O)_{1-5}$. *J. Chem. Phys.* **2003**, *119* (1), 187−194.

(28) Rienstra-Kiracofe, J. C.; Tschumper, G. S.; Schaefer, H. F.; Nandi, S.; Ellison, G. B. Atomic and Molecular Electron Affinities: Photoelectron Experiments and Theoretical Computations. *Chem. Rev.* **2002**, *102* (1), 231−282.

(29) Billes, F.; Mikosch, H.; Holly, S. A comparative study on the vibrational spectroscopy of pyridazine, pyrimidine and pyrazine. *J. Mol. Struct.: THEOCHEM* **1998**, *423* (3), 225−234.

(30) Navarro, A.; Fernández-Gómez, M.; López-González, J. J.; Fernández-Liencres, M. P.; Martínez-Torres, E.; Tomkinson, J.; Kearley, G. J. Inelastic Neutron Scattering Spectrum and Quantum Mechanical Calculations on the Internal Vibrations of Pyrimidine. *J. Phys. Chem. A* **1999**, *103* (29), 5833−5840.

(31) Pouchert, C. J. *The Aldrich Library of FT-IR Spectra*; Aldrich: Milwaukee, WI, 1997; Vol. 2.

(32) Howard, A. A.; Tschumper, G. S.; Hammer, N. I. Effects of Hydrogen Bonding on Vibrational Normal Modes of Pyrimidine. *J. Phys. Chem. A* **2010**, *114* (25), 6803−6810.

(33) Howard, J. C.; Hammer, N. I.; Tschumper, G. S. Structures, Energetics and Vibrational Frequency Shifts of Hydrated Pyrimidine. *ChemPhysChem* **2011**, *12*, 3262−3273.

(34) Wright, A. M.; Howard, A. A.; Howard, J. C.; Tschumper, G. S.; Hammer, N. I. Charge Transfer and Blue Shifting of Vibrational Frequencies in a Hydrogen Bond Acceptor. *J. Phys. Chem. A* **2013**, *117*, 5435−5446.

(35) Wright, A. M.; Joe, L. V.; Howard, A. A.; Tschumper, G. S.; Hammer, N. I. Spectroscopic and computational insight into weak noncovalent interactions in crystalline pyrimidine. *Chem. Phys. Lett.* **2011**, *501* (4−6), 319−323.

(36) Coe, J. V.; Lee, G. H.; Eaton, J. G.; Arnold, S. T.; Sarkas, H. W.; Bowen, K. H.; Ludewigt, C.; Haberland, H.; Worsnop, D. R.

Photoelectron spectroscopy of hydrated electron cluster anions, $(H_2O)^-_{n=2-69}$. *J. Chem. Phys.* **1990**, *92* (6), 3980−3982.